Electronic Supplementary Material (ESI) for Inorganic Chemistry Frontiers.

Supplementary Information

for

Metal–BODIPY complexes: versatile photosensitizers for oxidizing amyloid-β peptides and modulating their aggregation profiles

Mingeun Kim,[a] Gajendra Gupta,*[b] Junseong Lee,[c] Chanju Na,[a] Jimin Kwak,[a] Yuxi Lin,[d] Young-Ho Lee,[d,e,f,g,h] Mi Hee Lim*[a] and Chang Yeon Lee*[b]

[a]Department of Chemistry, Korea Advanced Institute of Science and Technology (KAIST), Daejeon 34141, Republic of Korea

[b]Department of Energy and Chemical Engineering/Innovation Center for Chemical Engineering, Incheon National University, Incheon 22012, Republic of Korea

[c]Department of Chemistry, Chonnam National University, Gwangju 61186, Republic of Korea

[d]Biopharmaceutical Research Center, Korea Basic Science Institute (KBSI), Ochang, Chungbuk 28119, Republic of Korea

[e]Bio-Analytical Science, University of Science and Technology (UST), Daejeon 34113, Republic of Korea

[f]Graduate School of Analytical Science and Technology, Chungnam National University, Daejeon 34134, Republic of Korea

[g]Department of Systems Biotechnology, Chung-Ang University (CAU), Gyeonggi 17546, Republic of Korea

[h]Frontier Research Institute for Interdisciplinary Sciences (FRIS), Tohoku University, Sendai, Miyagi 980-8578, Japan

*To whom correspondence should be addressed: gjngupt@gmail.com, miheelim@kaist.ac.kr, and cylee@inu.ac.kr

Table of Contents

Experimental Section

	Material and Methods	S4
	Synthesis of **BDP**, **Ru-BDP**, and **Ir-BDP**	S4
	X-Ray Crystal Structure	S6
	Ultraviolet–Visible (UV–Vis) Spectroscopy	S6
	Photoluminescence Spectroscopy	S6
	Singlet Oxygen ($^1O_2$) Generation	S6
	Superoxide Anion Radicals ($O_2^{\bullet-}$) and Hydroxyl Radicals (•OH) Production	S7
	Isothermal Titration Calorimetry (ITC)	S7
	Preparation of Amyloid-β (Aβ)	S7
	Electrospray Ionization–Mass Spectrometry (ESI–MS)	S7
	Tandem MS (ESI–MS^2)	S8
	Aβ Aggregation Experiments	S8
	Gel Electrophoresis with Western Blotting (Gel/Western Blot)	S8
	Transmission Electron Microscopy (TEM)	S9
	Cell Culture and MTT Assay	S9
	Statistical Analysis	S10
Table S1	Crystallographic data and parameters from **Ru-BDP** and **Ir-BDP**	S11
Table S2	Selected bond lengths (Å) and angles (°) for **Ru-BDP** and **Ir-BDP**	S12
Fig. S1	^1H, ^{13}C, and ^{19}F NMR spectra of **BDP** in $CDCl_3$	S13
Fig. S2	Mass spectrometric data of **BDP**	S14
Fig. S3	^1H, ^1H-DOSY, ^{13}C, and ^{19}F NMR spectra of **Ru-BDP** in $CDCl_3$	S15
Fig. S4	Mass spectrometric data of **Ru-BDP**	S16
Fig. S5	^1H, ^1H-DOSY, ^{13}C, and ^{19}F NMR spectra of **Ir-BDP** in $CDCl_3$	S17
Fig. S6	Mass spectrometric data of **Ir-BDP**	S18
Fig. S7	Spectra of electronic absorption and photoluminescence of **BDP**, **Ru-BDP**, and **Ir-BDP**	S19
Fig. S8	Electronic absorption spectra of **BDP**, **Ru-BDP**, and **Ir-BDP**	S20
Fig. S9	Kinetic profile of the DHN absorbance in response to $^1O_2$ generation by **BDP**, **Ru-BDP**, and **Ir-BDP**	S21
Fig. S10	Identification of the oxidized sites in Aβ induced by	

	BDP, **Ru-BDP**, and **Ir-BDP**	S22
Fig. S11	Influence of **BDP**, **Ru-BDP**, and **Ir-BDP** on the aggregation of $A\beta_{42}$	S23
Fig. S12	Effects of **BDP**, **Ru-BDP**, and **Ir-BDP** on preformed Aβ aggregates	S24
Fig. S13	Cytotoxicity of **BDP**, **Ru-BDP**, and **Ir-BDP**	
	with or without light exposure in 5Y cells	S25
Fig. S14	Impact of **BDP**, **Ru-BDP**, and **Ir-BDP** on the cytotoxicity induced by Aβ	S26
References		S27

Experimental Section

Materials and Methods. All reagents were purchased from commercial suppliers and used as received unless otherwise noted. Analyses of **BDP** and its metal complexes by nuclear magnetic resonance (NMR) spectroscopy and mass spectrometry (MS) were conducted on an Agilent 400-MR spectrometer [Santa Clara, CA, USA; Korea Basic Science Institute (KBSI), Republic of Korea] using the residual protonated solvent as internal standard and on a Waters Synapt G2S*i* spectrometer (Milford, MA, USA; KBSI), respectively. Amyloid-β_{40} ($A\beta_{40}$; DAEFRHDSGYEVHHQ-KLVFFAEDVGSNKGAIIGLMVGGVV) and $A\beta_{42}$ (DAEFRHDSGYEVHHQKLVFFAEDVGSNKGAI-IGLMVGGVVIA) were obtained from Peptide Institute, Inc. (Osaka, Japan). HEPES {2-[4-(2-hydroxyethyl)piperazin-1-yl]ethanesulfonic acid} was purchased from Sigma-Aldrich (St. Louis, MO, USA). The buffered solution was prepared in doubly distilled water [ddH_2O; a Milli-Q Direct 16 system (18.2 MW·cm; Merck KGaA, Darmstadt, Germany)]. Trace metal contamination was removed from the solutions by treating them with Chelex (Sigma-Aldrich) overnight. Absorption and luminescence spectra were recorded on a Thermo Scientific Genesys 10S ultraviolet–visible (UV–Vis) spectrometer (Waltham, MA, USA) and a Horiba Scientific Fluoromax spectrometer (Kyoto, Japan), respectively. KL 1500 compact SCHOTT (150-watt halogen cold light; Mainz, Germany) and PR160L Kessil lamp (525 nm; Kessil Lighting, Richmond, CA, USA) were used for light exposure of samples. Isothermal titration calorimetry (ITC) measurements were performed using the VP–ITC instrument (Malvern Panalytical Ltd., Malvern, UK; KBSI, Ochang, Republic of Korea). Mass spectrometric analysis of the interactions with $A\beta$ in the absence and presence of **BDP**, **Ru-BDP**, **Ir-BDP**, and light was conducted by an Agilent 6530 AccurateMass quadrupole time-of-flight liquid chromatography/mass spectrometry. Images gained by gel electrophoresis with Western blotting (gel/Western blot) were visualized by a ChemiDoc MP imaging system (Bio-Rad, Hercules, CA, USA). Transmission electron microscopic images were taken by a Tecnai F20 transmission electron microscope [FEI; KAIST Analysis Center for Research Advancements (KARA), Daejeon, Republic of Korea]. A SpectraMax M5e microplate reader (Molecular Devices, Sunnyvale, CA, USA) was used to measure the absorbance for the MTT assay [MTT = 3-(4,5-dimethylthiaol-2-yl)-2,5-diphenyltetrazolium bromide].

Synthesis of **BDP**, **Ru-BDP**, and **Ir-BDP**

*Preparation of **BDP**.* 1,3,5-benzenetricarbonyl trichloride (1.325 g, 0.005 mmol) was dissolved in dry dichloromethane (CH_2Cl_2; 100 mL) under N_2 (g). Then, 2,4-dimethyl pyrrole (2.85 g, 0.031 mmol) was added to the solution and stirred at room temperature for 12 h. Triethylamine

(TEA; 15 mL) and boron trifluoride etherate ($BF_3 \cdot OEt_3$; 15 mL) were added dropwise simultaneously at 0 °C and mixed at room temperature for 9 h. The reaction mixture was extracted with saturated aqueous NaCl solution. The CH_2Cl_2 layer was collected and evaporated under a vacuum. The crude residue was purified by column chromatography on silica gel using a mixture of petroleum ether:ethyl acetate = 4:1 followed by CH_2Cl_2 as eluent. The eluent contains products with one and two-**BODIPY** groups, which was further separated using dichloromethane:hexane mixture by slowly decreasing the hexane fraction (red powder; 615 mg, yield = 22%). ^{1}H NMR [400 MHz, $CDCl_3$, δ (ppm)]: 9.88 (2H, s), 8.06 (1H, s), 7.79 (2H, s), 6.03 (2H, s), 5.89 (2H, s), 2.58 (6H, s), 2.31 (6H, s), 2.00 (6H, s), 1.54 (6H, s). ^{13}C NMR [100 MHz, $CDCl_3$, δ (ppm)]: 183.40, 156.12, 142.52, 141.10, 139.52, 137.26, 135.40, 131.21, 131.00, 130.56, 129.23, 127.41, 121.67, 113.48, 15.20, 14.59, 13.14. ^{19}F NMR [376 MHz, $CDCl_3$, δ (ppm)]: –146.14 (2F, q). ESI–MS: *m/z* Calcd. for $C_{33}H_{34}BF_2N_4O_2$ $[M + H]^+$: 567.2742; found: 567.2741, $C_{33}H_{33}BF_2N_4O_2Na$ $[M + Na]^+$: 589.2562; found: 589.2562.

*Preparation of **Ru-BDP**.* **BDP** (30 mg, 0.053 mmol) and potassium *tert*-butoxide (*t*-BuOK; 12 mg, 0.107 mmol) were dissolved in a dried mixture of methanol:dichloromethane = 1:1 (12 mL), and N_2 (g) was bubbled through the solution for few min. The reaction mixture was stirred for 1 h. After adding (cymene)ruthenium dichloride dimer (32.4 mg, 0.053 mmol) to the reaction, it was stirred for 24 h. The reaction mixture was filtered by cotton-packed celite to remove undissolved particles. Diethyl ether was slowly added to the solution and kept at room temperature for slow evaporation. After 2 or 3 d, crystal structures suitable for X-ray crystallography were formed and dried under vacuum (dark brown powder; 45 mg, yield = 77%). ^{1}H NMR [400 MHz, $CDCl_3$, δ (ppm)]: 7.85 + 7.77 (1H, s), 7.57 (2H, s), 6.00 (4H, m), 5.63 (2H, t, *J* = 8 Hz), 5.58 (4H , m), 5.31 (2H, d, *J* = 8 Hz), 2.69 (2H, sept, *J* = 8 Hz), 2.57 (12H, m), 2.29 (6H, m), 1.95, (3H, s), 1.88 (3H, s), 1.46 (6H, m), 1.18 (6H, t, *J* = 8 Hz), 1.12 (6H, t, *J* = 8 Hz). ^{13}C NMR [100 MHz, $CDCl_3$, δ (ppm)]: 181.73, 154.44, 142.51, 138.13, 137.42, 135.89, 134.54, 121.49, 119.84, 100.94, 98.81, 83.54, 82.76, 80.78, 31.16, 22.26, 18.94, 17.79, 15.11, 14.61. ^{19}F NMR [376 MHz, $CDCl_3$, δ (ppm)]: –146.39 (2F, q). ESI–MS: *m/z* Calcd. for $C_{43}H_{46}BF_2N_4O_2Ru$ [M – *p*-cymeneRuCl – Cl]$^+$: 801.2725; found: 801.2714, $C_{53}H_{60}BClF_2N_4O_2Ru_2$ $[M – Cl]^+$: 1072.2553; found: 1071.2474.

*Preparation of **Ir-BDP**.* The synthetic process for **Ir-BDP** is similar to that for **Ru-BDP**. Instead of using (cymene)ruthenium dichloride dimer, pentamethylcyclopentadienyl iridium dimer (42.2

mg, 0.053 mmol) was added to the reaction mixture (dark brown powder; 48 mg, yield = 70%). ^{1}H NMR [400 MHz, $CDCl_3$, δ (ppm)]: 8.08 + 7.92 (1H, s), 7.71 (2H, d), 6.08 (2H, m), 5.98 (2H, m), 2.53 (12H, m), 2.14 (3H s), 2.03 (3H, s), 1.69 (30H, s), 1.55 (6H, m). ^{13}C NMR [100 MHz, $CDCl_3$, δ (ppm)]: 182.56, 182.19, 155.86, 152.59, 142.08, 139.15, 137.60, 137.36, 136.60, 136.35, 134.94, 134.06, 130.71, 121.48, 119.18, 84.59, 17.14, 14.61, 9.30. ^{19}F NMR [376 MHz, $CDCl_3$, δ (ppm)]: –146.38 (2F, q). ESI–MS: *m/z* Calcd. for $C_{43}H_{46}BF_2IrN_4O_2$ [M – Cp*IrCl – Cl]$^+$: 892.3311; found: 893.3387, $C_{53}H_{61}BClF_2Ir_2N_4O_2$ [M – Cl]$^+$: 1255.3802; found: 1255.3785.

X-Ray Crystal Structure. Reflection data for **Ru-BDP** and **Ir-BDP** were collected using a Bruker APEX-II CCD-based diffractometer with graphite-monochromated MoKα radiation (λ = 0.7107 Å). The hemisphere of the reflection data was collected as ω scan frames at 0.5 °/frame and an exposure time of 5 s/frame. The cell parameters were determined and refined using the APEX2 program.[1] The data were corrected for Lorentz and polarization effects, and an empirical absorption correction was applied using the SADABS program.[2] The **BDP**-based metal complexes were solved by direct methods and refined by full-matrix least-squares using the SHELXTL program package[3] and Olex2[4] with anisotropic thermal parameters for all non-hydrogen atoms. The relevant data are summarized in Table S1. CCDC 2299411 (**Ru-BDP**) and 2299412 (**Ir-BDP**) contain the supplementary crystallographic data for this study. These data can be obtained free of charge from The Cambridge Crystallographic Data Centre *via* www.ccdc.cam.ac.uk/data_request/cif.

UV–Vis Spectroscopy. The electronic absorption of **BDP** and its metal complexes in solution was monitored at room temperature by UV–Vis spectroscopy. **BDP**, **Ru-BDP**, and **Ir-BDP** (10 μM) were added in $CHCl_3$ or water (1% DMSO).

Photoluminescence Spectroscopy. Luminescence spectra of **BDP** and its metal complexes (10 μM) in $CHCl_3$ or water (1% DMSO) were measured by fluorometer at room temperature.

$^{1}O_2$ Generation. The amount of singlet oxygen ($^{1}O_2$) produced upon treatment of **BDP**, **Ru-BDP**, or **Ir-BDP** (5 μM) was determined by 1,5-dihydroxynaphthalene (DHN; 10 μM) in $CHCl_3$.[5,6] Dioxygen gas was passed into the DHN and photosensitizer solution for *ca.* 10 min. Subsequently, 3 mL of photosensitizer was added to 10 mL of DHN solution. The light was continuously irradiated while stirring from a distance of 8–10 cm. 3 mL of the solution was taken out each time, and

absorbance was measured continuously at regular intervals.

$O_2^{\bullet-}$ and •OH Production. BDP, **Ru-BDP**, and **Ir-BDP** were prepared at a concentration of 10 μM. A stock solution of dihydrorhodamine 123 (DHR 123 for detecting $O_2^{\bullet-}$) or terephthalic acid (TA for monitoring •OH) was prepared at 10 mM in DMSO and subsequently diluted to obtain a working solution of 10 μM. DHR 123 or TA was slowly added to **BDP**, **Ru-BDP**, and **Ir-BDP** in a 1:1 volume ratio. The resulting mixture was irradiated with light for 10 min, and the change in the emission intensity was observed immediately after irradiation (λ_{ex} = 485 nm and 310 nm for the DHR 123 and TA assays, respectively).

ITC. The solutions of Aβ$_{40}$ and **BDP**, **Ru-BDP**, and **Ir-BDP** were subjected to degassing under vacuum for 3 min prior to loading into the instrument. The solution of **BDP** (50 μM), **Ru-BDP** (100 μM), and **Ir-BDP** (150 μM) [20 mM HEPES, pH 7.4 (3% v/v DMSO, 0.0036% w/w NH_4OH)] in the syringe was titrated into the solution containing Aβ$_{40}$ [2.5 μM (for **BDP**), 5 μM (for **Ru-BDP**), and 7.5 μM (for **Ir-BDP**); 20 mM HEPES, pH 7.4 (3% v/v DMSO, 0.0036% w/w NH_4OH)] in the cell at 10 °C with 25 injections at a constant interval of 360 s (2 μL for the first injection and 11 μL for the following injections). The cell was continuously stirred at 307 rpm. The initial delay and the reference power were 60 s and 10 μcal/s, respectively. Dilution heat was also measured under the same experimental conditions. The ITC thermogram and binding isotherm were shown after the subtraction of the dilution heat. The binding isotherm after baseline correction was fitted to the one-set-of-sites binding model using the MicroCal Origin 7.0 software.

Preparation of Aβ. Aβ samples were prepared following previously reported procedures.[7-9] Aβ was dissolved in ammonium hydroxide [1% w/w NH_4OH (aq)]. The resulting solution was aliquoted, lyophilized overnight, and stored at –80 °C. The stock solution of Aβ was then prepared by dissolving the peptide using 1% w/w NH_4OH (aq) (10 μL) and diluting it with ddH_2O. The concentration of the samples was determined by measuring the absorbance of the solution at 280 nm (ε = 1,450 $M^{-1}cm^{-1}$ for Aβ$_{40}$; ε = 1,490 $M^{-1}cm^{-1}$ for Aβ$_{42}$).

ESI–MS. Aβ (100 μM) was incubated with **BDP**, **Ru-BDP**, and **Ir-BDP** (100 μM; 1% v/v DMSO) in 100 mM ammonium acetate, pH 7.4 for 1 h at 37 °C with constant agitation. For the illuminated samples, PR160L Kessil lamp (525 nm, Kessil Lighting) was applied for 10 min prior to incubation. The incubated samples were diluted by 10-fold with H_2O and then injected into the mass

spectrometer. The capillary voltage, nozzle voltage, and gas temperature were set to 5.8 kV, 2 kV, and 300 °C, respectively.

ESI–MS^2. The singly, doubly, and triply oxidized Aβ_{40} species generated with light-activated **BDP**, **Ru-BDP**, and **Ir-BDP** were further analyzed by tandem MS. ESI parameters and experimental conditions were the same as the ESI–MS methods. Collision-induced dissociation (CID) was carried out by applying the collision energy in the trap ranging from 63 to 65 V. More than 200 spectra were obtained for each sample and averaged for the analysis.

Aβ Aggregation Experiments. Aβ samples were prepared in 20 mM HEPES, pH 7.4, 150 mM NaCl. For the inhibition studies, **BDP**, **Ru-BDP**, and **Ir-BDP** (final concentration, 10 μM; 1% v/v DMSO) were added to the samples of Aβ (10 μM) followed by incubation for 24 h at 37 °C with constant agitation. For the disaggregation studies, Aβ (10 μM) was incubated for 24 h at 37 °C with constant agitation to generate preformed Aβ aggregates. The resulting Aβ aggregates were then treated with **BDP**, **Ru-BDP**, and **Ir-BDP** (10 μM) and incubated for an additional 24 h with constant agitation. For the illuminated samples, a PR160L Kessil lamp (525 nm, Kessil Lighting) was applied for 10 min prior to 24 h incubation. For the experiments under anaerobic conditions, all samples were prepared following the same procedure described above for the aerobic samples with glass tubes in the N_2 (g)-filled glovebox.

Gel/Western Blot. The resultant Aβ species from the inhibition and disaggregation experiments were analyzed by gel/Western blot using anti-Aβ antibodies (6E10, Covance, Princeton, NJ, USA; anti-Aβ 22-35, Sigma-Aldrich).[10-13] The samples (10 μL) were separated on a 10–20% Tris-tricine gel (Invitrogen, Carlsbad, CA, USA). Following separation, the peptides were transferred onto nitrocellulose membranes and blocked with bovine serum albumin (BSA; 3% w/v; Sigma-Aldrich) in Tris-buffered saline (TBS) containing 0.1% v/v Tween-20 (Sigma-Aldrich) (TBS-T) for 4 h at room temperature or overnight at 4 °C. The membranes were incubated with 6E10 (1:2,000; Covance) or anti-Aβ 22-35 (1:10,000; Sigma-Aldrich) in a solution of BSA (2% w/v in TBS-T) for 2 h at room temperature or overnight at 4 °C. After washing with TBS-T (three times, 10 min), a horseradish peroxidase (HRP)-conjugated goat anti-mouse secondary antibody (for 6E10; 1:5,000 in 2% w/v BSA in TBS-T; Cayman Chemical Company, Ann Arbor, MI, USA) or HRP-conjugated goat anti-rabbit secondary antibody (for anti-Aβ 22-35; 1:5,000 in 2% w/v BSA in TBS-T; Invitrogen) was added for 2 h at room temperature. Lastly, a homemade ECL kit[10,11,14] was

used to visualize gel/Western blots on a ChemiDoc MP Imaging System (Bio-Rad).

TEM. Samples for TEM were prepared according to the previously reported methods with slight modifications.[7,8] Glow-discharged grids (Formvar/Carbon 300-mesh, Electron Microscopy Sciences, Hatfield, PA, USA) were treated with the samples of Aβ (5.5 μL, 10 μM) for 2 min at room temperature. Excess samples were removed using filter paper and by washing once with ddH_2O. Each grid incubated with uranyl acetate (5.5 μL, 1% w/v in ddH_2O) for 1 min was blotted off and dried overnight at room temperature. Images for each sample were taken on a transmission electron microscope (200 kV; 29,000x magnification). For the TEM measurements, we randomly selected locations of samples on the grids for imaging and collected at least 25 images from each grid.

Cell Culture and MTT assay. The human neuroblastoma SH-SY5Y (5Y) cell line was purchased from the American Type Culture Collection (ATCC, VA, USA). The cell line was maintained in media containing 50% v/v minimum essential medium (GIBCO, NY, USA) and 50% v/v F12 (GIBCO), and supplemented with 10% v/v fetal bovine serum (Sigma-Aldrich), 100 U/mL penicillin, and 100 mg/mL streptomycin (GIBCO). Cells were grown and maintained at 37 °C in a humidified atmosphere with 5% CO_2. The cells used for our studies did not indicate mycoplasma contamination. Cell viability upon treatment with **BDP**, **Ru-BDP**, and **Ir-BDP** was determined by the MTT assay. Two types of samples were prepared: cytotoxicity of (i) **BDP**, **Ru-BDP**, and **Ir-BDP** with and without light exposure and (ii) Aβ. Cells were seeded in a 96-well plate for both experiments (10,000 cells in 100 μL per well). To identify the cell viability of **BDP**, **Ru-BDP**, and **Ir-BDP** and ROS generated by light-activated them, the cells were treated with their various concentrations (1, 2.5, 5, and 10 μM; 1% v/v DMSO) without and with light illumination for 10 min and then incubated for 24 h at 37 °C. For two experiments with Aβ, (i) Aβ (10 μM) was added with **BDP**, **Ru-BDP**, and **Ir-BDP** (1, 2.5, 5, and 10 μM; 1% v/v DMSO) exposed to the PR160L Kessil lamp (520 nm, Kessil Lighting) for 10 min, and the resultant Aβ species were treated with cells, and (ii) Aβ (10 μM) was pre-treated with cells, followed by the addition of **BDP**, **Ru-BDP**, and **Ir-BDP** (1, 2.5, 5, and 10 μM; 1% v/v DMSO) and photoactivation with the PR160L Kessil lamp (520 nm, Kessil Lighting) for 10 min. After 24 h incubation, MTT [25 μL of 5 mg/mL in phosphate-buffered saline (PBS; pH 7.4; GIBCO)] was added to each well, and the plate was incubated for 4 h at 37 °C. Formazan produced by cells was solubilized using an acidic solution of dimethylformamide (pH 4.5, 50% v/v, aq) and sodium dodecyl sulfate (20% w/v) overnight at room

temperature in the dark. The absorbance was measured at 600 nm by a microplate reader. Cell viability was calculated relative to that of the cells containing an equivalent amount of DMSO or the buffered solution. All measurements were conducted in triplicate.

Statistical Analysis. The comparison between the two groups was performed with Student's *t*-test. Values were denoted as mean ± s.e.m. Statistical difference was considered significant at $*P < 0.05$, $**P < 0.01$, or $***P < 0.001$.

Table S1 Crystallographic data and parameters from **Ru-BDP** and **Ir-BDP**.

	Ru-BDP	**Ir-BDP**
Identification code	Inu50-1	Inu49-1
CCDC #	2299412	2299411
Empirical formula	$C_{53.8}H_{60.61}BCl_{3.61}F_2N_4O_2Ru_2$	$C_{53}H_{60}BCl_2F_2Ir_2N_4O_2$
Formula weight	1174.16	1289.16
Temperature/K	100	100
Crystal system	monoclinic	monoclinic
Space group	$P2_1/n$	$P2_1/n$
a/Å	12.8846(5)	15.1069(4)
b/Å	22.2271(9)	21.8645(5)
c/Å	18.3548(6)	15.7566(4)
α/°	90	90
β/°	92.285(2)	90.6914(16)
γ/°	90	90
Volume/Å^3	5252.4(3)	5204.1(2)
Z	4	4
ρ_{calc}g/cm^3	1.485	1.645
μ/mm^{-1}	0.810	5.262
F(000)	2399.0	2532.0
Crystal size/mm^3	0.1 x 0.1 x 0.1	0.1 x 0.1 x 0.1
Radiation	MoKα (λ = 0.71073)	MoKα (λ = 0.71073)
2θ range for data collection/°	3.792 to 50.798	4.154 to 50.774
Index ranges	-15 ≤ h ≤ 15, -26 ≤ k ≤ 26, -22 ≤ l ≤ 22	-18 ≤ h ≤ 18, -26 ≤ k ≤ 26, -18 ≤ l ≤ 18
Reflections collected	68708	67017
Independent reflections	9627 [R_{int} = 0.1203, R_{sigma} = 0.0952]	9517 [R_{int} = 0.1028, R_{sigma} = 0.0720]
Data/restraints/parameters	9627/155/730	9517/85/619
Goodness-of-fit on F^2	1.029	1.043
Final R indexes [I≥2σ (I)]	R_1 = 0.0656, wR_2 = 0.1476	R_1 = 0.0830, wR_2 = 0.1990
Final R indexes [all data]	R_1 = 0.1191, wR_2 = 0.1716	R_1 = 0.1204, wR_2 = 0.2215
Largest diff. peak/hole/e Å^{-3}	2.10/-0.84	9.42/-2.40

$R_1 = \sum||Fo| - |Fc||/\sum|Fo|$; $wR_2 = \{[\sum w(Fo^2 - Fc^2)^2]/[\sum w(Fo^2)^2]\}^{1/2}$.

Table S2 Selected bond lengths (Å) and angles (°) for **Ru-BDP** and **Ir-BDP**.

Ru-BDP		**Ir-BDP**	
Ru1–N1	2.017	Ir1–N1	2.031
Ru1–O1	2.084	Ir1–O1	2.111
Ru1–Cl1	2.401	Ir1–Cl1	2.400
Ru2–N2	2.052	Ir2–N2	2.059
Ru2–O2	2.101	Ir2–O2	2.122
Ru2–Cl2	2.394	Ir2–Cl2	2.401
B1–F1	1.390	B1–F1	1.414
B1–F2	1.377	B1–F2	1.380
B1–N3	1.542	B1–N3	1.574
B1–N4	1.546	B1–N4	1.523
O1–Ru1–Cl1	88.10	O1–Ir1–Cl1	87.44
O2–Ru2–Cl2	88.11	O2–Ir2–Cl2	87.31
O1–Ru1–N1	78.17	O1–Ir1–N1	77.40
O2–Ru2–N2	77.90	O2–Ir2–N2	77.65
N3–B1–N4	106.51	N3–B1–N4	106.54
F1–B1–F2	110.27	F1–B1–F2	108.44

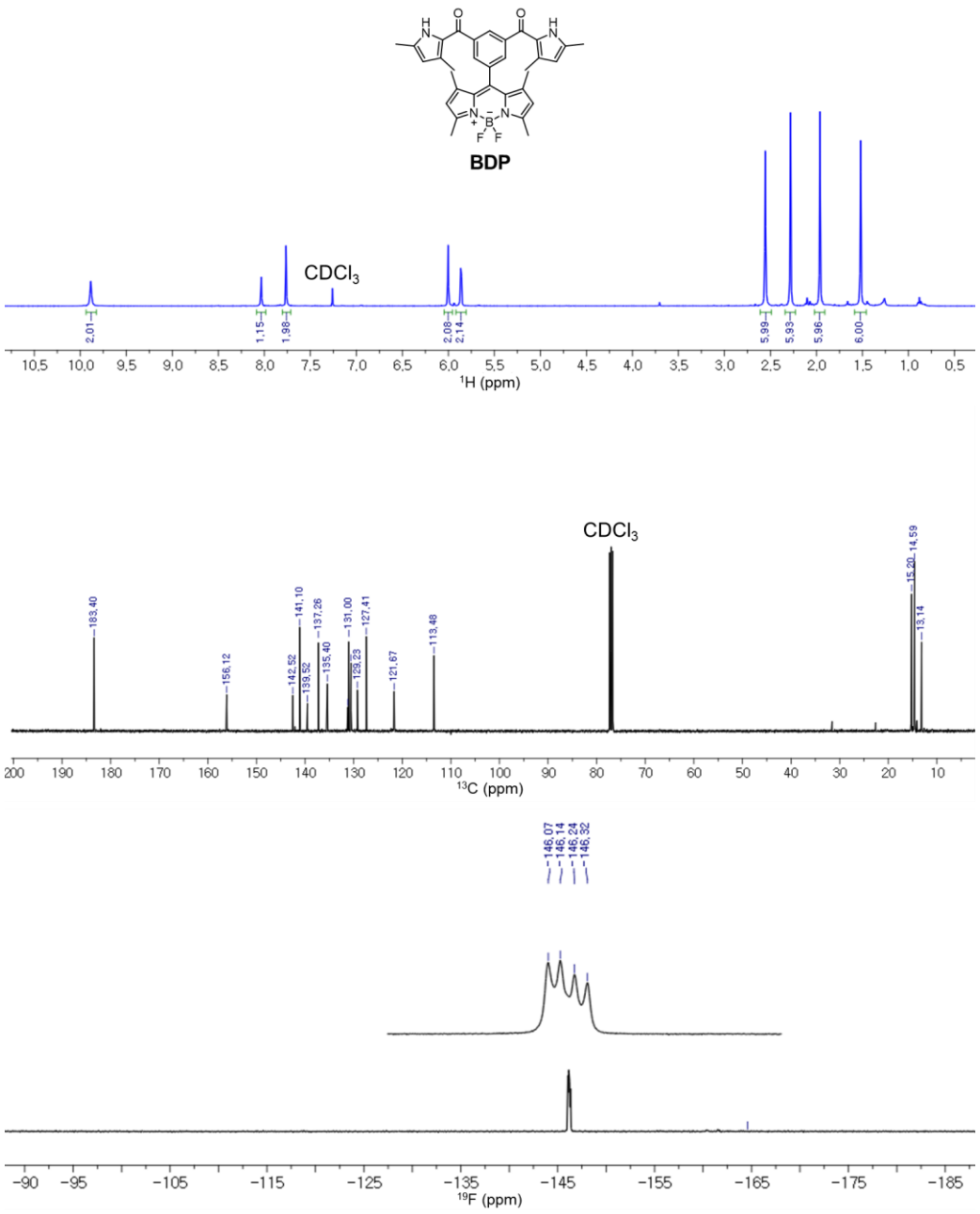

Fig. S1 ^{1}H, ^{13}C, and ^{19}F NMR spectra of **BDP** in $CDCl_3$.

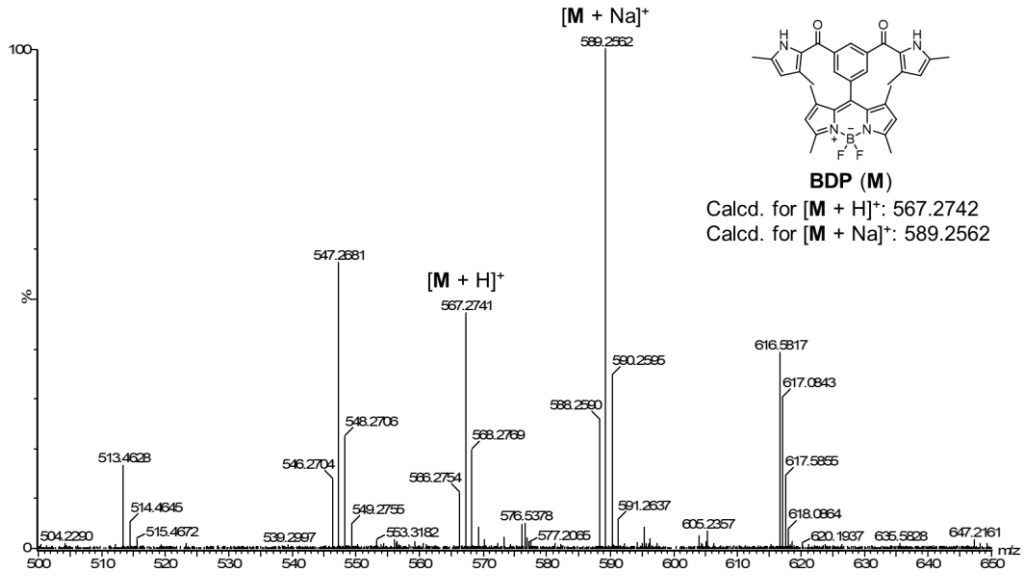

Fig. S2 Mass spectrometric data of **BDP**.

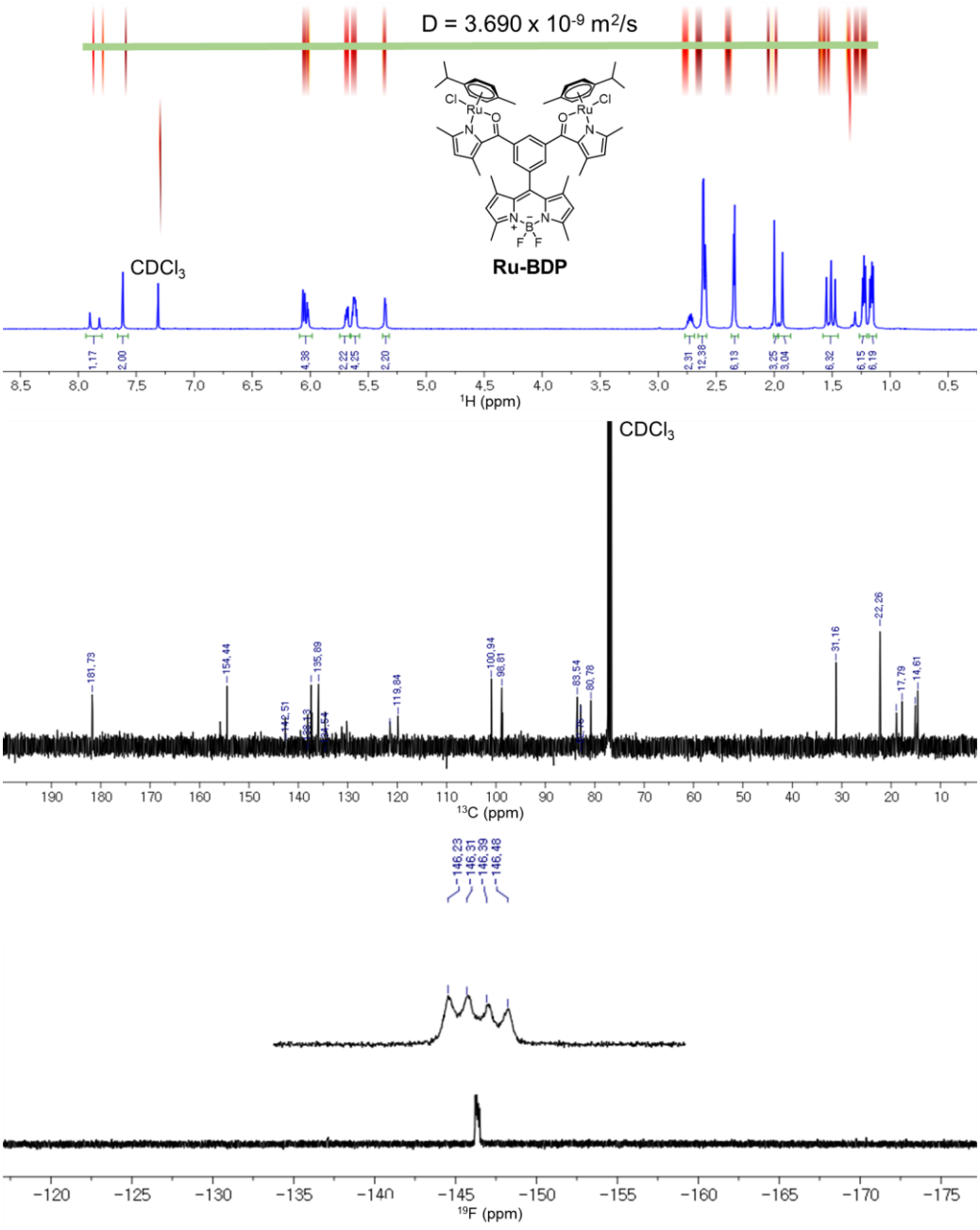

Fig. S3 ^{1}H, ^{1}H-DOSY, ^{13}C, and ^{19}F NMR spectra of **Ru-BDP** in $CDCl_3$.

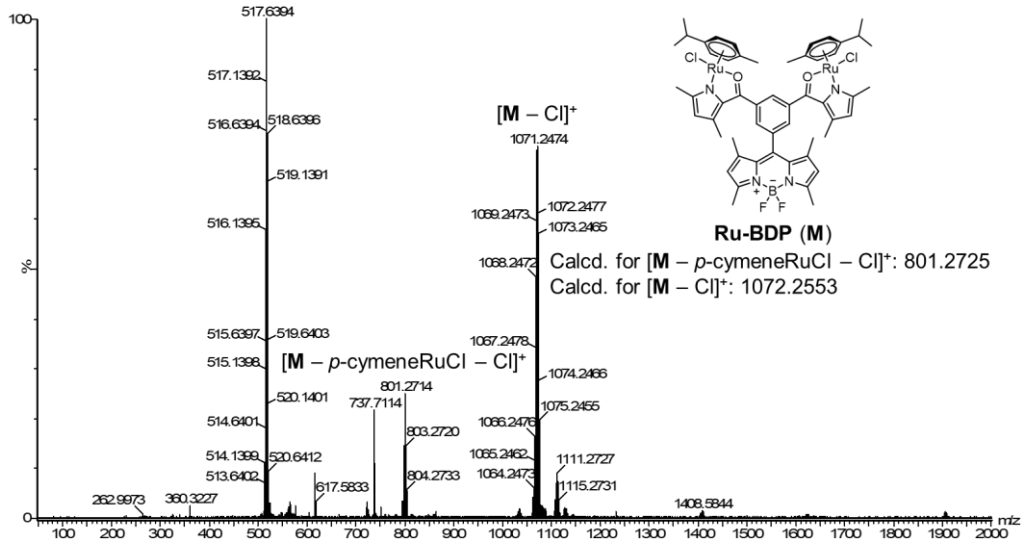

Fig. S4 Mass spectrometric data of **Ru-BDP**.

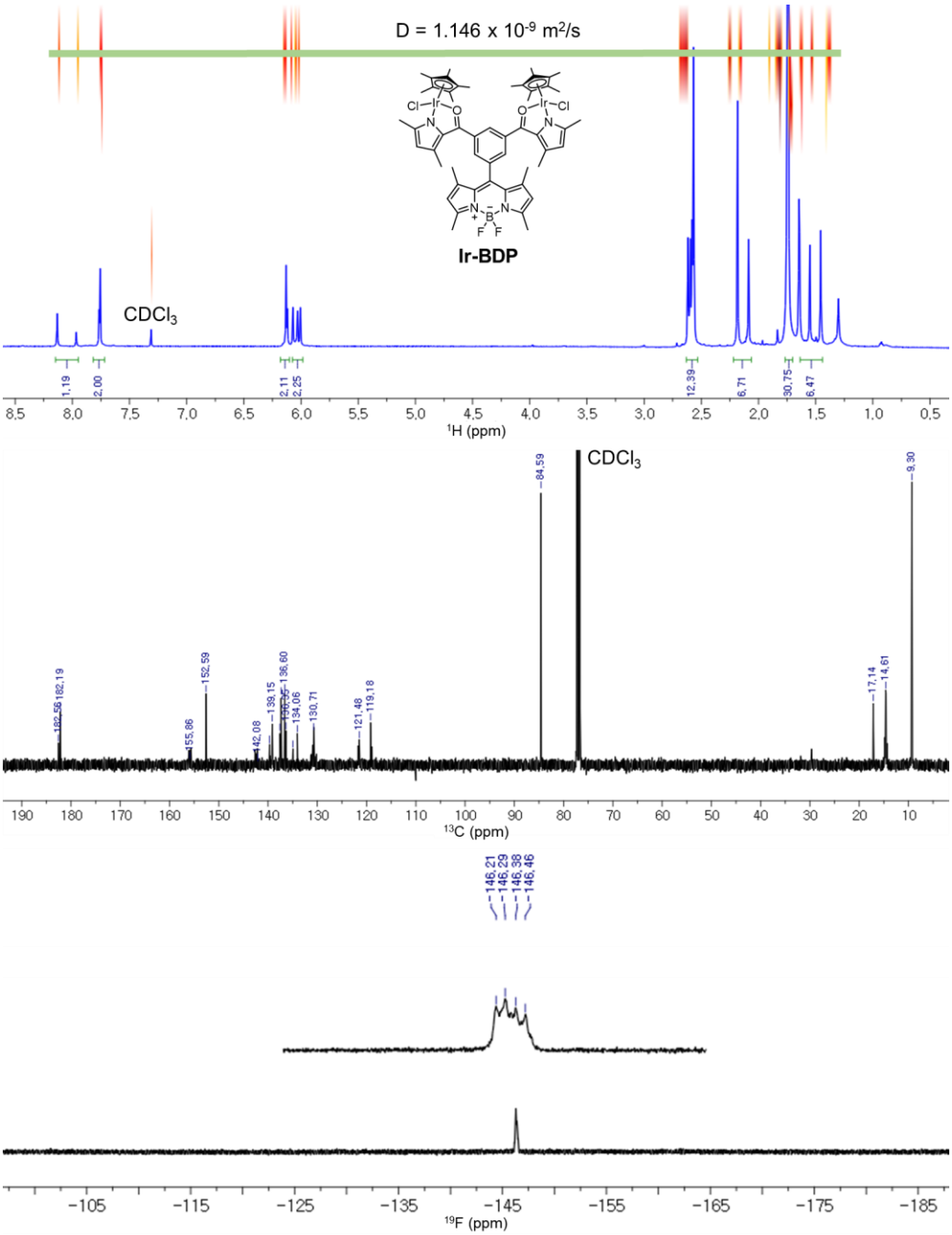

Fig. S5 ^{1}H, ^{1}H-DOSY, ^{13}C, and ^{19}F NMR spectra of **Ir-BDP** in $CDCl_3$.

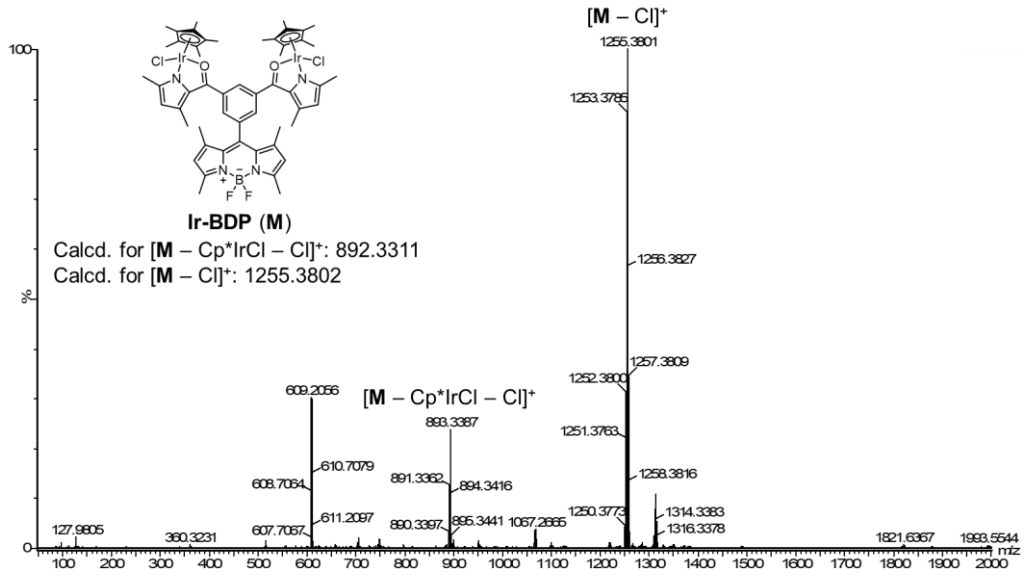

Fig. S6 Mass spectrometric data of **Ir-BDP**.

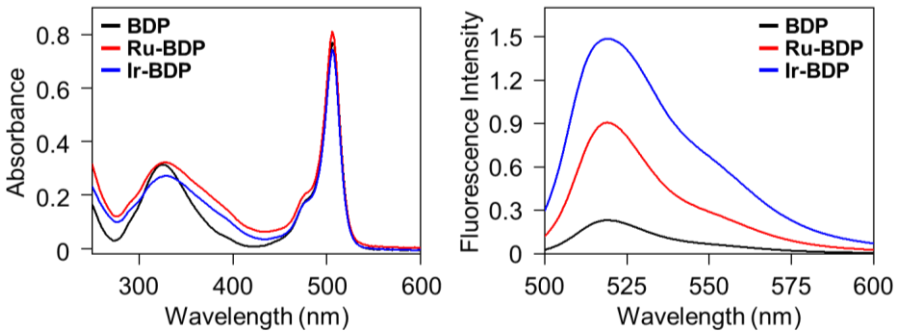

Fig. S7 Spectra of electronic absorption and photoluminescence of **BDP**, **Ru-BDP**, and **Ir-BDP**. Conditions: [**BDP**, **Ru-BDP**, and **Ir-BDP**] = 10 μM; $CHCl_3$; room temperature.

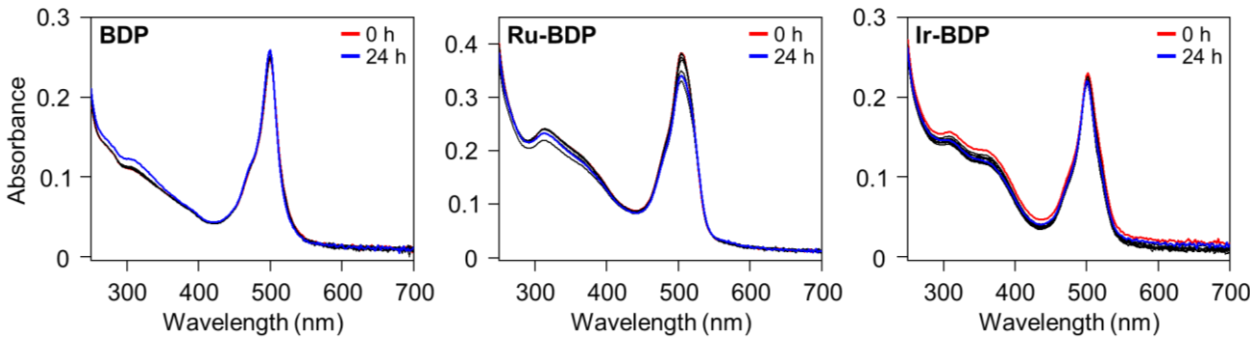

Fig. S8 Electronic absorption spectra of **BDP**, **Ru-BDP**, and **Ir-BDP**. Conditions: [**BDP**, **Ru-BDP**, and **Ir-BDP**] = 10 μM; water (1% v/v DMSO); room temperature; 0–24 h.

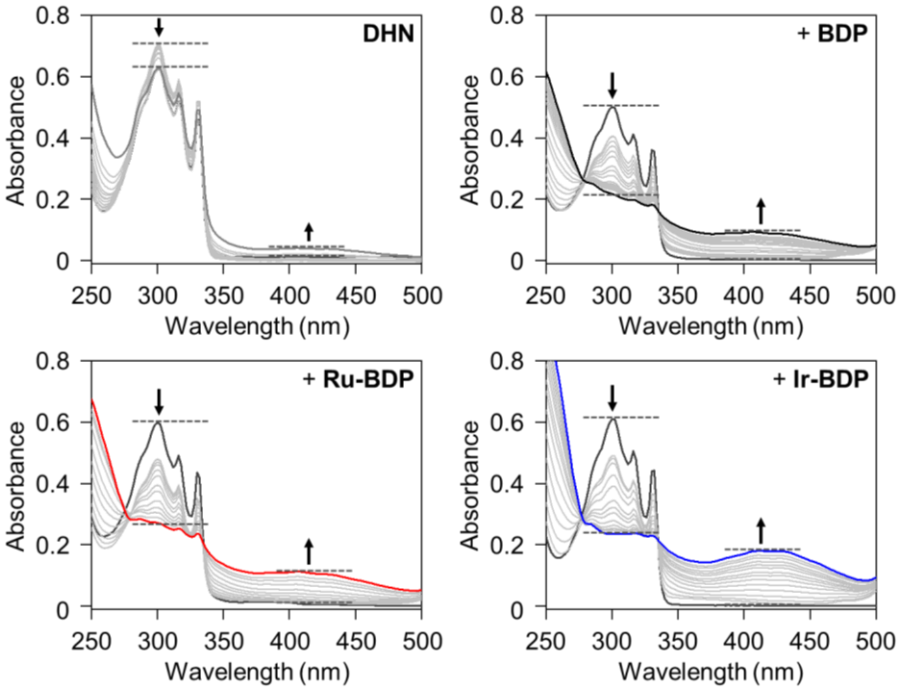

Fig. S9 Kinetic profile of the DHN absorbance in response to $^1O_2$ generation by **BDP**, **Ru-BDP**, and **Ir-BDP**. Conditions: [**BDP**, **Ru-BDP**, and **Ir-BDP**] = 5 μM; [DHN] = 10 μM; $CHCl_3$; room temperature; 150-watt halogen cold light.

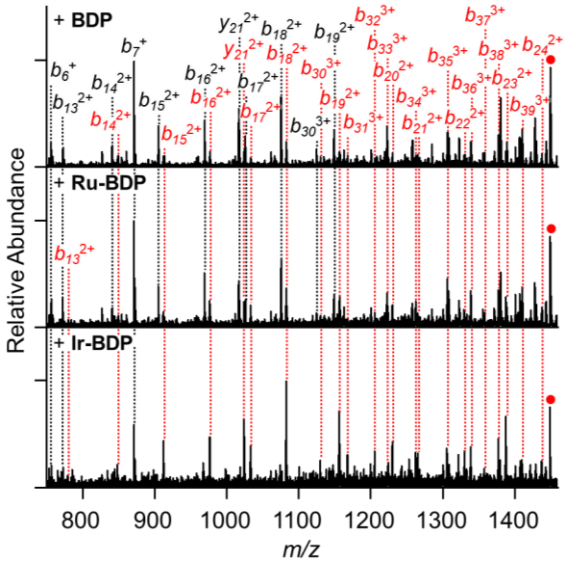

Fig. S10 Identification of the oxidized sites in Aβ induced by **BDP**, **Ru-BDP**, and **Ir-BDP**. (a) Analysis of singly oxidized peaks in $A\beta_{40}$ by ESI–MS^2 upon incubation with **BDP**, **Ru-BDP**, and **Ir-BDP**. Monooxidized *b* (*N*-terminal fragment ions) or *y* (*C*-terminal fragment ions) fragments are indicated in red. Conditions: [$A\beta_{40}$] = 100 μM; [**BDP**, **Ru-BDP**, and **Ir-BDP**] = 100 μM; 100 mM ammonium acetate, pH 7.4; 37 °C; 1 h; 250 rpm; Kessil lamp (525 nm) for 10 min. The samples were diluted by 10-fold with H_2O before injection into the mass spectrometer.

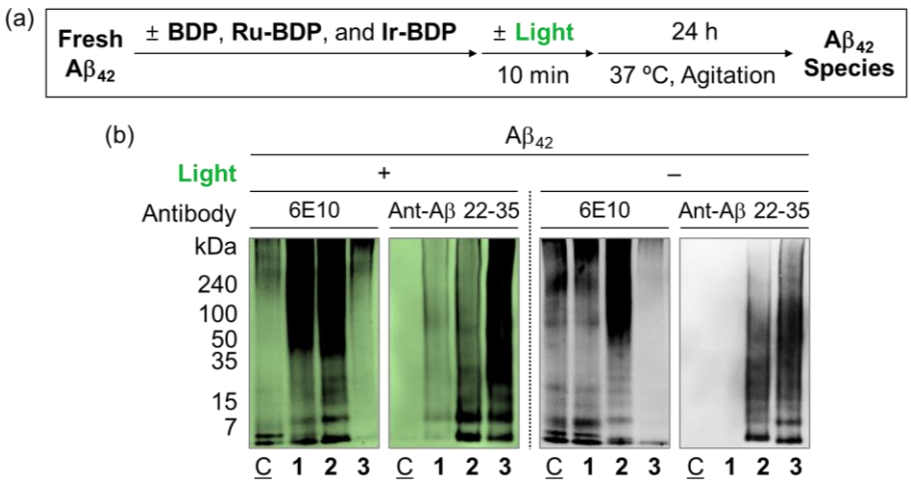

Fig. S11 Influence of **BDP**, **Ru-BDP**, and **Ir-BDP** on the aggregation of $A\beta_{42}$. (a) Scheme of the inhibition experiment. (b) Analysis of the resultant $A\beta_{42}$ species through gel/Western blot with two antibodies (*e.g.*, 6E10 and anti-Aβ 22-35) with and without **BDP**, **Ru-BDP**, **Ir-BDP**, and light. Lanes: (C) $A\beta_{42}$; (**1**) $A\beta_{42}$ + **BDP**; (**2**) $A\beta_{42}$ + **Ru-BDP**; (**3**) $A\beta_{42}$ + **Ir-BDP**. Conditions: [$A\beta_{42}$] = 10 μM; [**BDP**, **Ru-BDP**, and **Ir-BDP**] = 10 μM; 20 mM HEPES, pH 7.4, 150 mM NaCl; 37 °C; 24 h; 250 rpm; Kessil lamp (525 nm) for 10 min.

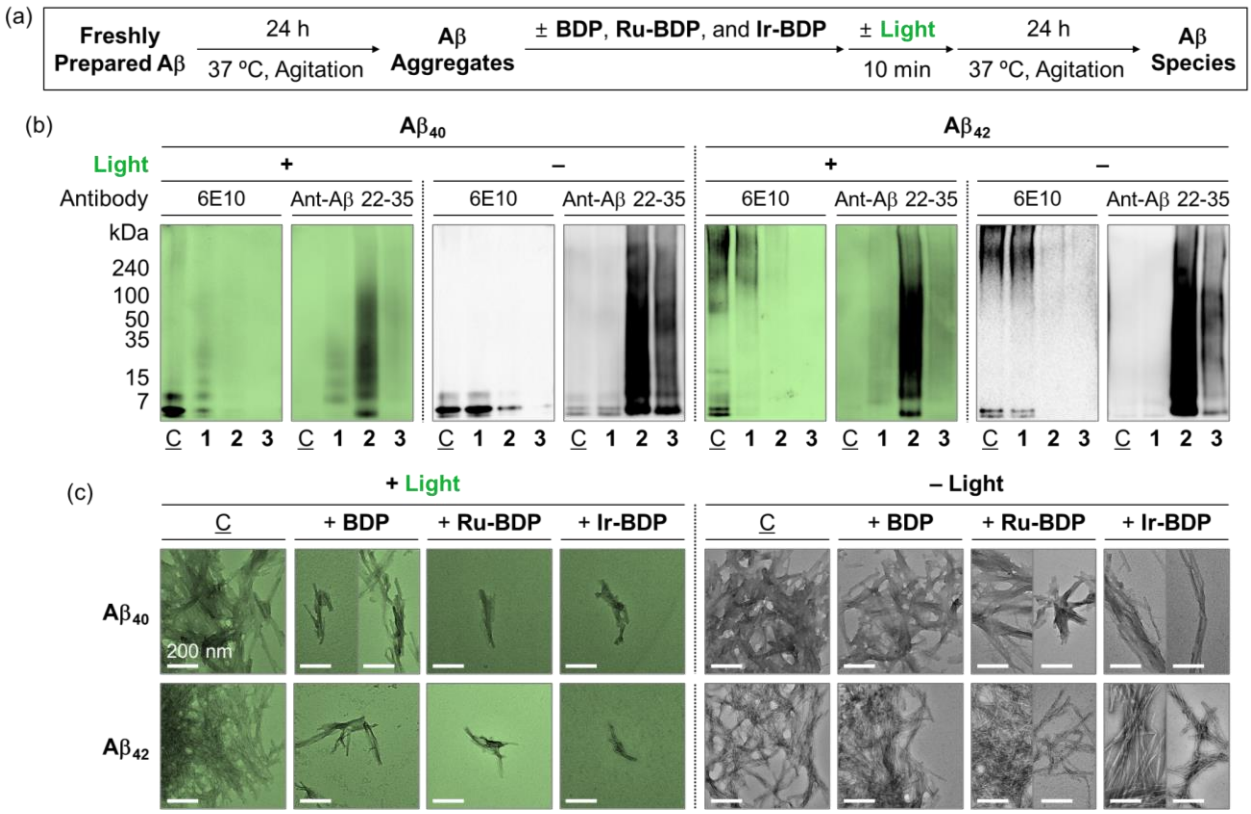

Fig. S12 Effects of **BDP**, **Ru-BDP**, and **Ir-BDP** on preformed Aβ aggregates. (a) Scheme of the disaggregation experiment. (b) Analysis of the resultant Aβ species through gel/Western blot with two antibodies (*e.g.*, 6E10 and anti-Aβ 22-35) with and without **BDP**, **Ru-BDP**, **Ir-BDP**, and light. Lanes: (C) Aβ; (**1**) Aβ + **BDP**; (**2**) Aβ + **Ru-BDP**; (**3**) Aβ + **Ir-BDP**. (c) TEM analysis of the morphologies of the resultant Aβ aggregates by incubation with **BDP**, **Ru-BDP**, and **Ir-BDP** with and without light exposure. Conditions: [Aβ] = 10 μM; [**BDP**, **Ru-BDP**, and **Ir-BDP**] = 10 μM; 20 mM HEPES, pH 7.4, 150 mM NaCl; 37 °C; 24 h; 250 rpm; Kessil lamp (525 nm) for 10 min. Scale bar = 200 nm.

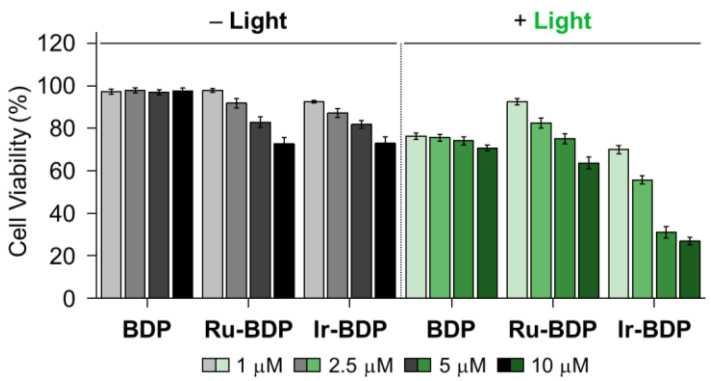

Fig. S13 Cytotoxicity of **BDP**, **Ru-BDP**, and **Ir-BDP** with or without light exposure in 5Y cells. Cell survival (%) determined by the MTT assay was calculated, compared to that of cells treated with an equivalent amount of DMSO (1% v/v DMSO). Conditions: [**BDP**, **Ru-BDP**, and **Ir-BDP**] = 1, 2.5, 5, and 10 μM; 20 mM HEPES, pH 7.4, 150 mM NaCl; 37 °C; Kessil lamp (525 nm) for 10 min. All values are indicated as mean ± s.e.m.

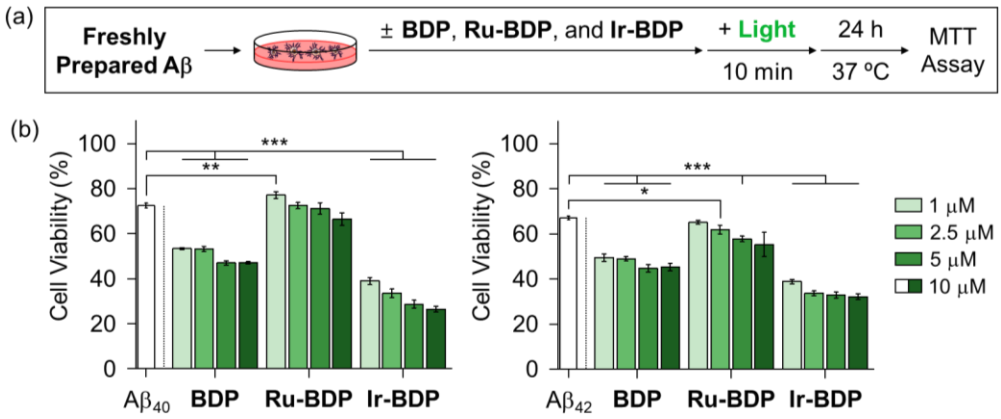

Fig. S14 Impact of **BDP**, **Ru-BDP**, and **Ir-BDP** on the cytotoxicity induced by Aβ. (a) Scheme of the cell studies. (b) Cell viability (%) of 5Y cells incubated with Aβ followed by treatment of **BDP**, **Ru-BDP**, and **Ir-BDP** and photoactivation. Cell survival (%) measured by the MTT assay was calculated, relative to that of cells treated with an equivalent amount of the buffered solution. Conditions: [Aβ] = 10 μM; [**BDP**, **Ru-BDP**, and **Ir-BDP**] = 1, 2.5, 5, and 10 μM; 20 mM HEPES, pH 7.4, 150 mM NaCl; 37 °C; Kessil lamp (525 nm) for 10 min. All values are indicated as mean ± s.e.m. $^{*}P < 0.05$, $^{**}P < 0.01$, or $^{***}P < 0.001$ by a two-sided unpaired Student's *t*-test.

References

1. Bruker-AXS (2014). APEX2. Version 2014.11-0. Madison, Wisconsin, USA.
2. L. Krause, R. Herbst-Irmer, G. M. Sheldrick and D. Stalke, Comparison of silver and molybdenum microfocus X-ray sources for single-crystal structure determination, *J. Appl. Crystallogr.*, 2015, **48**, 3-10
3. G. Sheldrick, Crystal structure refinement with SHELXL, *Acta Cryst. C*, 2015, **71**, 3-8.
4. O. V. Dolomanov, L. J. Bourhis, R. j. Gildea, J. A. K. Howard and H. Puschmann, OLEX2: a complete structure solution, refinement and analysis program, *J. Appl. Crystallogr.*, 2009, **42**, 339-341.
5. W. Wu, P. J. Yang, L. Ma, J. Lalevée and J. Zhao, Visible-light harvesting Pt^{II} complexes as singlet oxygen photosensitizers for photooxidation of 1,5-dihydroxynaphthalene, *Eur. J. Inorg. Chem.*, 2012, **2013**, 228-231.
6. S.-y. Takizawa, R. Aboshi and S. Murata, Photooxidation of 1,5-dihydroxynaphthalene with iridium complexes as singlet oxygen sensitizers, *Photochem. Photobiol. Sci.*, 2011, **10**, 895-903.
7. M. Hong, M. Kim, J. Yoon, S.-H. Lee, M.-H. Baik and M. H. Lim, Excited-state intramolecular hydrogen transfer of compact molecules controls amyloid aggregation profiles, *JACS Au*, 2022, **2**, 2001-2012.
8. J. Kang, J. S. Nam, H. J. Lee, G. Nam, H.-W. Rhee, T.-H. Kwon and M. H. Lim, Chemical strategies to modify amyloidogenic peptides using iridium(III) complexes: coordination and photo-induced oxidation, *Chem. Sci.*, 2019, **10**, 6855-6862.
9. J. Kang, S. J. C. Lee, J. S. Nam, H. J. Lee, M.-G. Kang, K. J. Korshavn, H.-T. Kim, J. Cho, A. Ramamoorthy, H.-W. Rhee, T.-H. Kwon and M. H. Lim, An Iridium(III) complex as a photoactivatable tool for oxidation of amyloidogenic peptides with subsequent modulation of peptide aggregation, *Chem. Eur. J.*, 2017, **23**, 1645-1653.
10. M. Kim, J. Kang, M. Lee, J. Han, G. Nam, E. Tak, M. S. Kim, H. J. Lee, E. Nam, J. Park, S. J. Oh, J.-Y. Lee, J.-Y. Lee, M.-H. Baik and M. H. Lim, Minimalistic principles for designing small molecules with multiple reactivities against pathological factors in dementia, *J. Am. Chem. Soc.*, 2020, **142**, 8183-8193.
11. J. S. Derrick, R. A. Kerr, Y. Nam, S. B. Oh, H. J. Lee, K. G. Earnest, N. Suh, K. L. Peck, M. Ozbil, K. J. Korshavn, A. Ramamoorthy, R. Prabhakar, E. J. Merino, J. Shearer, J.-Y. Lee, B. T. Ruotolo and M. H. Lim, A redox-active, compact molecule for cross-linking amyloidogenic peptides into nontoxic, off-pathway aggregates: *in vitro* and *in vivo* efficacy and molecular mechanisms, *J. Am. Chem. Soc.*, 2015, **137**, 14785-14797.

12. L. P. Feilen, S.-Y. Chen, A. Fukumori, R. Feederle, M. Zacharias and H. Steiner, Active site geometry stabilization of a presenilin homolog by the lipid bilayer promotes intramembrane proteolysis, *eLife*, 2022, **11**, e76090.
13. X. Zhang, Y.-J. Gou, Y. Zhang, J. Li, K. Han, Y. Xu, H. Li, L.-H. You, P. Yu, Y.-Z. Chang and G. Gao, Hepcidin overexpression in astrocytes alters brain iron metabolism and protects against amyloid-β induced brain damage in mice, *Cell Death Discov.*, 2020, **6**, 113.
14. D. D. Mruk and C. Y. Cheng, Enhanced chemiluminescence (ECL) for routine immunoblotting: an inexpensive alternative to commercially available kits, *Spermatogenesis*, 2011, **1**, 121-122.